Chalcogenide Letters Vol. 20, No. 6, June 2023, p. 399 - 407

The effect of the concentration of tin (Sn) in the metallic precursor, on the structure, morphology, optical and electrical properties of electrochemically deposited lead-tin-sulphide (PbSnS) thin films

I. Nkrumah*, F. K. Ampong, A. Britwum, M. Paal, B. Kwakye-Awuah,
R. K. Nkum, F. Boakye
Department of Physics, Kwame Nkrumah University of Science and Technology, Kumasi, Ghana

A study has been carried out to investigate the effect of the concentration of Sn in the metallic precursor on the structure, morphology, optical and electrical properties of PbSnS thin films. The films were directly electrodeposited on ITO-coated glass substrates using a 3-electrode electrochemical cell having graphite as the counter electrode and Ag/AgCl as the reference electrode. Several depositions were carried out, with each deposited film having a different concentration of Sn in the metallic precursor whilst all other parameters were kept constant for all the films. Post deposition annealing was carried out in air at 250 ^{o}C for an hour. A variety of techniques were used to characterize the films. Results showed that the increase in Sn concentration did not modify the structure and preferred orientation of the films. However, it caused a slight increase in the average grain size of the films and electrical conductivity. All the films showed direct transition with the optical band gap reducing with increasing Sn concentration. The refractive index of the films showed anomalous dispersion behaviour within the UV region, and normal dispersion in the visible and infrared regions, whilst following an increasing trend with the grain size. SEM image showed spherically shaped grains of different sizes distributed randomly with good coverage across the entire area of the substrate. The EDAX spectrum was consistent with formation of the ternary PbSnS compound on ITO-coated glass substrate. Overall results indicate that, the optical and electrical properties of the electrochemically deposited PbSnS thin films can be tuned to make them suitable for specific applications by varying the concentration of Sn in the metallic precursor.

(Received March 23, 2023; Accepted June 6, 2023)

Keywords: Lead tin sulphide thin films, Electrodeposition, Electrical properties, Optical properties

1. Introduction

The search for new materials for fabricating optoelectronic devices with improved efficiency, has generated considerable interest among scientists and researchers. Tin sulphide (SnS) and lead (PbS) are two of such materials which have been widely studied because of their favourable physical properties. In addition, the constituent elements of both materials are earth abundant with relatively lower extraction costs hence, given the additional advantage to lower the cost of device fabrication [1].

SnS is a potential absorber layer for solar cells due to its direct optical band gap of 1.75 eV [2], high absorption coefficient ($\alpha \approx 104$ cm^{-1} near the fundamental edge), and high hole mobility of 90 cm^3 V^{-1} S^{-1} [3]. SnS semiconductors can have p or n-type conductivity depending on the deposition conditions and doping materials. Recently, Nair et al. [4] combined orthorhombic SnS and cubic SnS as absorbers and achieved an efficiency of 1.38 %. Additionally, doping is an effective method for altering the physical properties of semiconductor materials [2]. The substitutional doping of Pb can improve the crystalline quality, and its high absorption capability can improve the optical absorption of SnS [5].

* Corresponding author: inkrumah.sci@knust.edu.gh
https://doi.org/10.15251/CL.2023.206.399

PbS, on the other hand, is the most studied material, among the group IV–VI compound semiconductors because of its potential applications in nonlinear optical devices [6]. It has been recommended as an earth abundant sustainable material for affordable photovoltaic devices [7]. PbS has a narrow direct band gap of 0.41 eV at room temperature and an optical absorption coefficient of 10^5 cm^{-1} [8]. Both p-type and n-type PbS compounds can be made by doping [9].

The ternary PbSnS which is relatively uncommon in literature, is now a material of significant interest. This material is easily formed due to the high miscibility of these two binary compounds PbS and SnS [10].

Such mixed thin film structures offer the advantage of tuneable optical and opto-electronic properties to suite a particular application [6]. Properties such as, band gap (and, therefore, spectral sensitivity), electrical conductivity, and structural properties can be varied to make them suitable for applications such as solar cell, photochemical, lasers and thermoelectricity [11, 12]. The potential of PbSnS as an absorber layer for solar cells due to its favourable optical band gap has been reported by some researchers [1].

Depositions of ternary PbSnS thin films have been demonstrated by a variety of techniques based on either physical or chemical processes. Each of these techniques producing their own unique microstructure characteristics. Among these techniques, electrodeposition is an economical method to deposit large area thin films and can lead to the real mass-production of solar cells [13].

In our previous publication by Nkrumah et al. [14], we reported on the electrodeposition of single-phase lead tin sulphide (PbSnS) thin films on ITO-coated glass substrates. In this paper, we investigated the type of majority charge carrier, optical and structural properties,

The current study, extends this investigation further and examines how the concentration of Sn in the metallic precursor affects the structure, morphology, optical and electrical properties of electrochemically deposited PbSnS thin films.

2. Methodology

The procedure used for the electrodeposition of lead tin sulphide (PbSnS) thin films is described in Nkrumah et al. [14]. In this section we present a brief summary of this procedure.

A conventional three-electrode electrochemical cell was used with ITO-coated glass substrates as the working electrode, graphite as the counter electrode and Ag/AgCl as the reference electrode. The electrolyte was prepared from an aqueous mixture containing lead (II) nitrate, $Pb(NO_3)_2$, tin (II) chloride dehydrate, $SnCl_2.2H_2O$ and sodium thiosulphate (anhydrous) $Na_2S_2O_3$.

In a typical experiment, equal volumes (~30 mL) of 0.003 M $Pb(NO_3)_2$, 0.003 M $SnCl_2.2H_2O$ and 0.1 M $Na_2S_2O_3$ were mixed together in a 100 ml beaker. The pH was adjusted to 2.8 by adding a few drops of H_2SO_4, this was done to improve the adherence of the electrodeposits.

A direct compound electrodeposition was carried out using an Edaq 467 Potentiostat, at a constant potential of -1.3 V vs Ag/AgCl at room temperature (28 °C). A growth time of ~12 minutes was ensured during electrodeposition. Several depositions were carried out. The concentration of the Sn electrolyte in the metallic precursor used for each deposition was varied from 0.001 M to 0.005 M in incremental steps of 0.001 M and all other deposition parameters were kept constant.

After deposition, all the films were annealed in air at a temperature of 250 ^oC for an hour to improve their crystallinity before film characterization.

3. Results and discussion

3.1. X-ray diffraction analyses

A PANalytical Empyrean Series 2 powder X-ray diffractometer with a Cu-kα radiation was used for the X-ray diffraction studies. The equipment was operated at 40 mA and 45 kV for phase analysis using the Bragg-Brentano geometry in the 2θ range 10 to 90 °. Total analysis time

per samples was around 35 minutes for a 2θ scan step of 0.06 °. Data treatment and analysis were carried out using high score plus software packages.

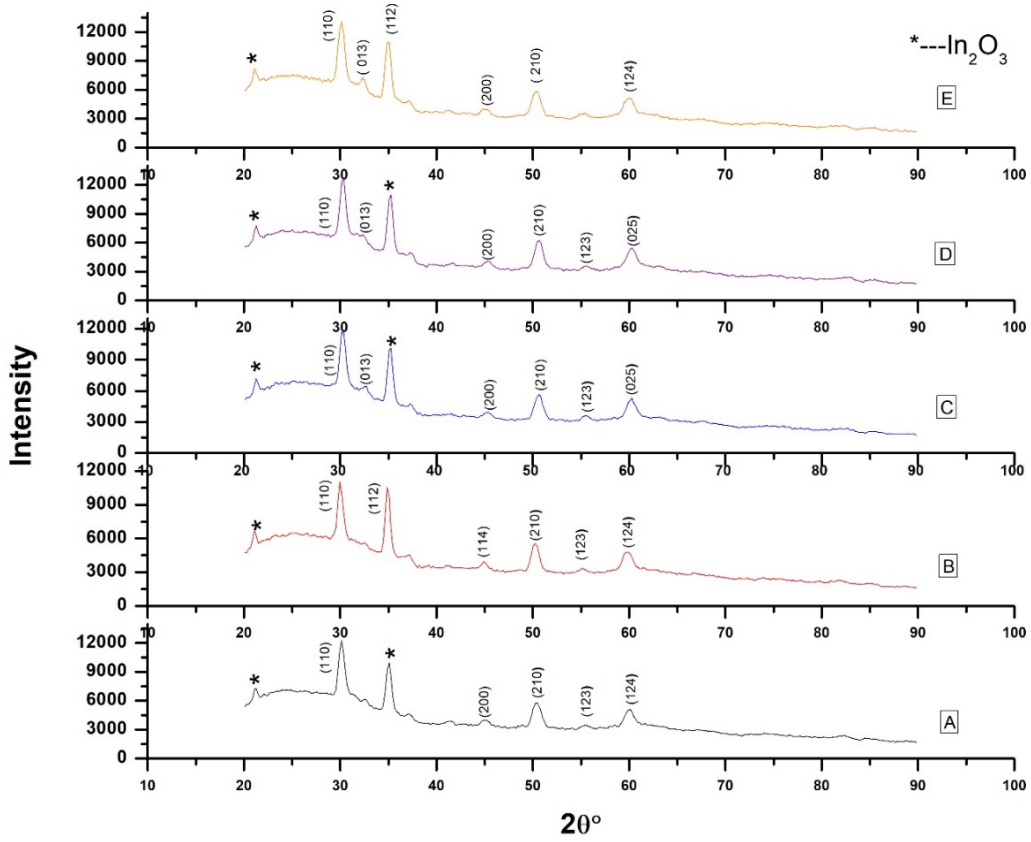

Fig. 1 shows the XRD patterns of the PbSnS films obtained at various concentrations of Sn

The different samples with the concentration of Sn being 0.001, 0.002, 0.003, 0.004, and 0.005 M had the corresponding labels A, B, C, D and E.

From figure 1, all the films exhibited the orthorhombic phase of PbSnS (Ref.Code. 98-015-6131). There were no structural variations observed in the films after varying the concentration of Sn in the metallic precursor. A slight increase in the intensity of the most intense peak indexed to the (110) plane was observed suggesting further grain growth along this direction with increasing Sn concentration. No other phases of PbSnS are observed in the diffractogram of figure 1. The few impurity peaks in the diffractogram labeled with asterisks are indexed to diindium trioxide which may emanate from the ITO-coated glass substrate. A typical pattern list generated from the XRD analyses is shown in table 1

Table 1. Shows the pattern list for the sample with 0.002 M concentration of Sn in the metallic Precursor.

Ref. Code	Score	Compound Name	Displ.[°2θ]	Scale Fac.	Chem. Formula
98-016-9432	61	Diindium Trioxide	0.000	0.901	In_2O_3
98-006-8969	26	Lead Sulfide	0.000	1.618	Pb_1S_1
98-015-6131	12	Lead Tin Sulfide (0.5/0.5/1)	0.000	0.178	$Pb_{0.5}S_1Sn_{0.5}$

The pattern list in table 1 confirms the composition of the deposit on the ITO-coated glass substrate.

3.2. Average grain size

The size of the crystalline particles at different concentrations of Sn is given by the Scherrer [15, 16] formula which is given as:

$$D = \frac{K\lambda}{\beta \cos\theta} \quad (1)$$

where D is the average grain size, λ is the X-ray wavelength, (0.15418 nm), β full width at half maximum (FWHM) or integral breadth, of the dominant peak and θ is the corresponding Bragg angle and K is the Scherrer constant. The results showed a significant increase in the grain size when the concentration of Sn changed from 0.001 M to 0.002 M, after which the increase in grain size was gradual. The table 2 below gives a summary of this variation

Table 2. Change in crystallite size with increasing Sn concentration.

Label	Concentration of Sn |(M)	Grain Size (nm)
A	0.001	11.081
B	0.002	14.773
C	0.003	14.781
D	0.004	14.782
E	0.005	14.788

3.3. Electrical characterization

The electrical conductivity was measured by a Jandel Four-Point Probe meter. The results of how the Sn concentration affects the electrical conductivity is shown in table 3.

Table 3. Electrical conductivity of the PbSnS films, varying in Sn concentration.

Sample	Concentration of Sn (M)	Conductivity Ω^{-1} cm^{-1}
1	0.001	0.0408
2	0.002	0.0419
3	0.003	0.0435
4	0.004	0.0432
5	0.005	0.0445

It can be seen from table 2 and 3, that when the Sn concentration in the metallic precursor increases, there is a corresponding increase in grain size and electrical conductivity of the films. Mkawi et al. [17] have explained that, an increase in grain size causes a reduction in the grain boundaries, thus effectively reducing the recombination of the charge carriers. This may ultimately result in an increase in conductivity of the films. Figure 2, shows a plot of electrical conductivity against samples of PbSnS with different concentrations of Sn in the metallic precursor.

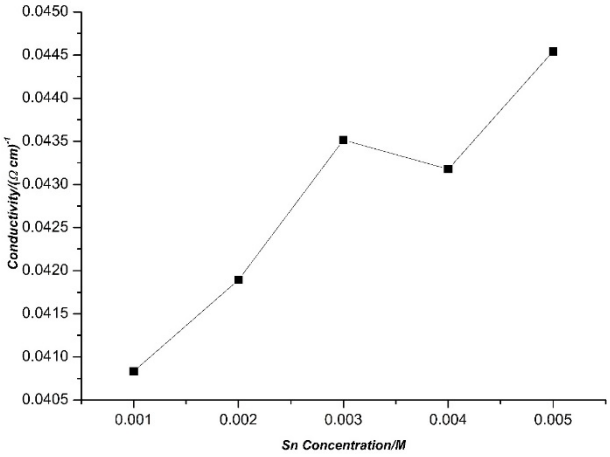

Fig. 2. Plot of electrical conductivity against samples of PbSnS with different concentrations of Sn in the metallic precursor.

Chalapathi et al. [2] have also suggested that in addition to grain size, the elemental composition also affects the electrical properties of the films. Thus, the observed increase in electrical conductivity with an increase in Sn concentration, could be attributed to the enhanced grain size and a slightly more Sn composition.

3.4. Scanning electron microscopy

The morphology and elemental composition of the samples was determined using a Thermo Scientific Axia ChemiSEM Scanning Electron Microscope.

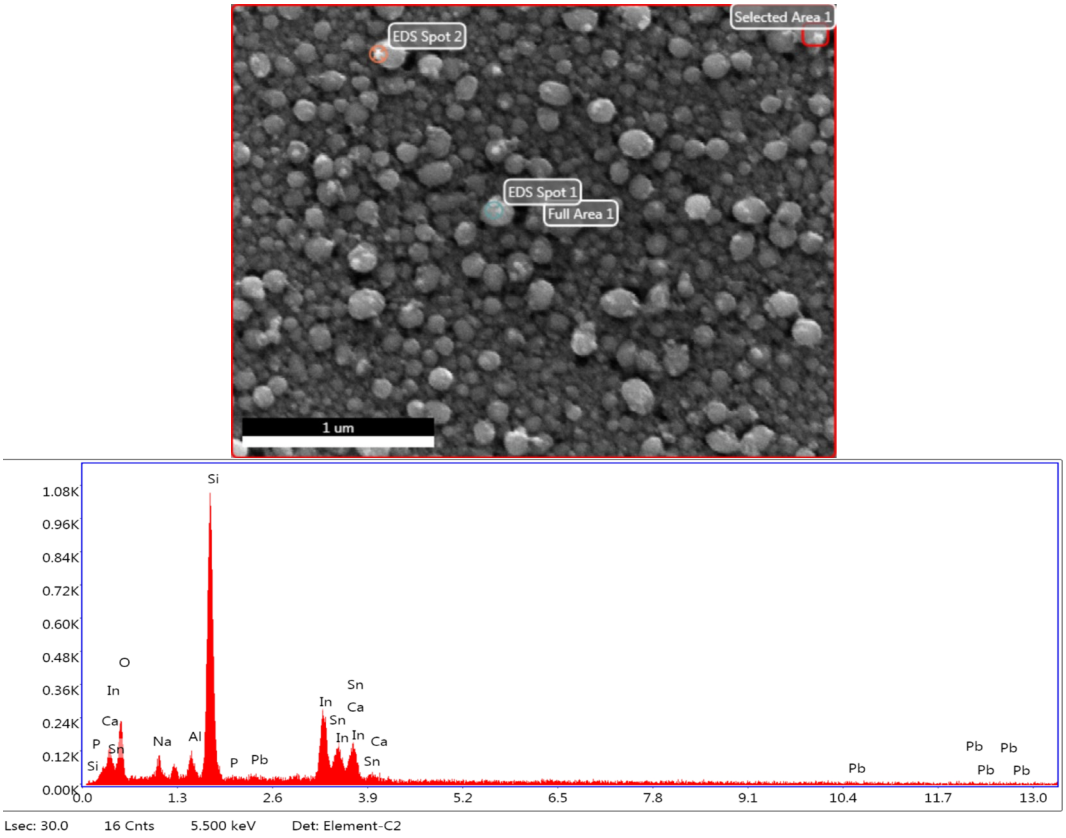

Fig. 3. (a) SEM image of the film with 0.004 M concentration of Sn in the metallic precursor; (b) EDAX spectrum of film with 0.004 M concentration of Sn in the metallic precursor.

Figure 3a shows the SEM image of the film with 0.004 M concentration of Sn in the metallic precursor. The image shows spherically shaped grains of different sizes distributed randomly on the substrate. Film appears compact with no pronounced voids and good coverage across the entire area of the substrate. All the films showed a similar morphology. Similar observations were made by Nkrumah et al. [14].

The spectrum in figure 3b is consistent with formation of the ternary PbSnS compound on ITO-coated glass substrate. The other elements such as Si, Ca, Mg and Al emanate from the substrate and the quantitative is shown in Table 4.

Table 4. Gives the quantitative results of the EDAX analysis of figure 3b.

Element	Weight%	Atomic%	Net Int	Error %	K ratio	Z	A	F
OK	25.23	46.22	53.38	12.94	0.0474	1.1566	0.1624	1.0000
NaK	5.14	6.55	19.89	15.80	0.0166	1.0559	0.3039	1.0035
NK	2.22	2.41	18.75	16.09	0.0127	1.0371	0.5460	1.0119
SiK	31.66	33.04	327.76	5.95	0.2206	1.0612	0.6533	1.0049
PK	0.00	0.00	0.03	99.99	0.0000	1.0205	0.5462	1.0084
PbM	0.65	0.09	2.10	78.50	0.0046	0.6865	1.0186	1.0120
lnl	25.79	6.58	92.48	7.83	0.2029	0.7785	1.0110	0.9996
Snl	3.52	0.87	11.06	34.69	0.0273	0.7662	1.0124	0.9994
CaK	5.78	4.23	37.49	13.77	0.0522	1.0081	0.8935	1.0022

3.5. Optical analysis

Generally, the optical properties of the semiconductors, especially the absorption spectra and optical band gaps, show profound sensitivity on the film microstructure. Any changes in the electronic structure of the material would be reflected in its optical behaviour [18].

3.5.1. Optical absorption

Optical absorption spectra were recorded with a Cecil CE7500 series double beam UV-Visible spectrometer operating at room temperature in the wavelength range of 190 nm to 1100 nm, a step height of 0.3 nm and a scan rate of 5 nm per second. The absorption spectra of the films are shown in figure 4.

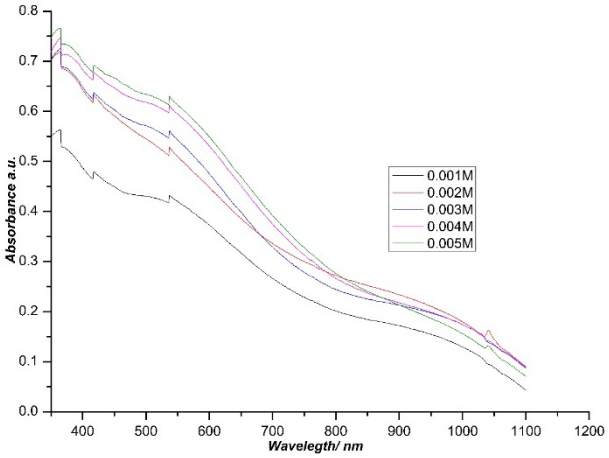

Fig. 4. Absorption spectra of PbSnS films for the different concentrations of Sn.

It can be observed from the optical spectra that there is a shift in the fundamental absorption edge towards longer wavelengths (red shift) with increasing Sn Concentration. This red

shift supports the view of an increase in grain size with a corresponding decrease in band gap [19] as the concentration of Sn is increased.

3.5.2. Energy band gap

The energy band gap and transition type was determined using the relationship given by the Stern equation [20], where ν is the frequency, h is the Planck's constant, K is a constant while n carries the value of either 1 for direct transition or 4 for indirect transition. Since SnS and PbS have direct transitions, it follows that their mixed compositions are also direct transitions, hence, n = 1.

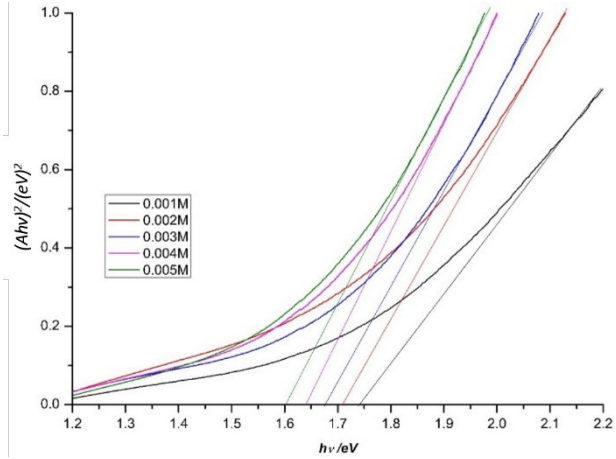

Fig. 5. Energy band gap for all compositions under investigation.

The energy band gap is obtained by plotting a line of best fit to the linear portion of the graph at high hν and extrapolating it to the point where it intersects the hν axis as shown in Figure 5. The optical band gap values were estimated to be 1.74, 1.70, 1.68, 1.64, and 1.60 eV the films with Sn concentration of 0.001 M, 0.002 M, 0.003 M, 0.004 M and 0.005 M respectively. This decrease in energy band gap is as a result of the increase in grain size thereby resulting in an increase in electrical conductivity as the concentration of Sn increases.

3.5.3. Refractive index

The refractive index 'n' of the thin films was calculated from the spectral data using the following relation.

$$n = \frac{1+\sqrt{R}}{1-\sqrt{R}} \tag{2}$$

where 'R' is the reflectance.

Figure 6 presents graphically the value of the refractive index for each wavelength in the range of 190 nm to 1100 nm. It can be observed that at lower values of wavelength, ($\lambda < 650$ nm) i.e., in the strong absorption region of the electromagnetic spectra, the refractive index values show anomalous (or resonant) dispersion behaviour [21]. After $\lambda \geq 680$ nm, which is from the visible to Infrared region, the refractive index decreases with wavelength and shows significant normal dispersion. Further observation shows that in this region, the refractive index 'n' of the films follows an increasing trend with the grain size.

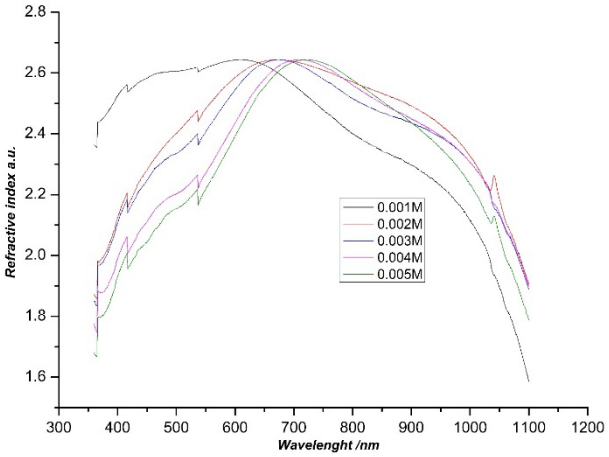

Fig. 6. Shows the spectral dependence of the refractive index for all compositions under investigation.

4. Conclusion

In this study the effect of the concentration of Sn in the metallic precursor on the structure, morphology, optical and electrical properties of PbSnS thin films grown by a single-step electrodeposition has been investigated. Results showed that the variation in Sn concentration did not modify the structure, however, the optical and electrical properties were altered. The increase in Sn concentration enhanced the crystallinity and increased the conductivity of the films whilst reducing the optical band gap. The refractive index of the films showed anomalous dispersion behaviour within the UV region, and normal dispersion in the visible and infrared regions, whilst following an increasing trend with the grain size. SEM micrographs showed a spherically shaped grains with different sizes covering the entire substrate with no cracks or pinholes. EDAX analysis of the film was consistent with the formation of PbSnS on ITO-coated substrates. Overall, the increase in Sn concentration caused an enhanced grain size, a reduced band gap, and improved the electrical properties of the films which could be beneficial for applications in thin film solar cells.

References

[1] J. Fang , D. D. Mishraa , W. Caib, G.Tana, Materials Science in Semiconductor Processing 68, 58 (2017); https://doi.org/10.1016/j.mssp.2017.06.015

[2] U. Chalapathi, Y. Jayasree, S. H. Park (2022), Materials Science in Semiconductor Processing 150, 10695 (2022); https://doi.org/10.1016/j.mssp.2022.106958

[3] J. Damisaa, J. O. Emeghaa, I. L. Ikhioya, J. Nig. Soc. Phys. Sci. 3, 455 (2021); https://doi.org/10.46481/jnsps.2021.157

[4] P. Nair, A. Garcia-Angelmo, M. Nair, Phys. Status Solidi A, 213 (1), 170 (2016); https://doi.org/10.1002/pssa.201532426

[5] S. Sebastian, I. Kulandaisamy, S. Valanarasu, I. Yahia, H.-S. Kim, D. Vikraman, J. Sol-Gel Sci. Technol. 93 (1), 52 (2020); https://doi.org/10.1007/s10971-019-05169-y

[6] F. G. Hone, F. K. Ampong, T. Abza, I. Nkrumah, R. K. Nkum, F. Boakye. Elixir Thin Film Tech. 76, 28432 (2014)

[7] I. Nkrumah, F. K. Ampong, B. Kwakye-Awauh, T. Ive, Journal of Advances in Physics 11 (1), 2954 (2015); https://doi.org/10.24297/jap.v11i1.6949

[8] M. Karabulut, H. Ertap, H. Mammadov, G. Ugurlu, M.K. Ozturk, Turkish Journal of Physics, 38 104 (2014); https://doi.org/10.3906/fiz-1301-1

[9] S.I. Sadovnikov, A.I. Gusev, Journal of Alloys and Compounds 573, 65 (2013);

https://doi.org/10.1016/j.jallcom.2013.03.290
[10] A. Łapińska, A. Taube, M. Wąsik, G. Z. Żukowska, A. Duzynska, J. Judeka and M. Zdrojek, J. Raman Spectrosc. 48, 479 (2016); https://doi.org/10.1002/jrs.5064
[11] L.P. Deshmukh, B. M. More, C.B. Rotti, G. S. Shashare, Materials Chemistry and Physics 45,145 (1996); https://doi.org/10.1016/0254-0584(96)80092-7
[12] A.K. Deb, V. Kumar, Physica Status Solidi B 254, 1600379-1 (2017); https://doi.org/10.1002/pssb.201600379
[13] J. A. Andrade-Arvizu, M. Courel-Piedrahita, O. Vigil-Galán, Journal of Materials Science: Materials in Electronics 26, 4541 (2015); https://doi.org/10.1007/s10854-015-3050-z
[14] I. Nkrumah, F. K. Ampong, A. Britwum, M. Paal, B. Kwakye-Awuah, R. K. Nkum, F.Boakye, Chalcogenide Letters 20(3), 205 (2023); https://doi.org/10.15251/CL.2023.203.205
[15] C. K. Bandoh, I. Nkrumah , F. K. Ampong, R. K. Nkum, F. Boakye, Chalcogenide Letters 18(2), 81 (2021); https://doi.org/10.15251/CL.2021.182.81
[16] M. Paal, I. Nkrumah, F. K. Ampong, D. U. Ngbiche, R. K. Nkum, F. Boakye, Science Journal of University of Zakho 8(3), 97 (2020); https://doi.org/10.25271/sjuoz.2020.8.3.752
[17] E. M. Mkawi, K. Ibrahim, M. K. M. Ali, A. S. Mohamed, Int. J. Electrochem. Sci 8, 359 (2013)
[18] O.V. Goncharova, V. F. Gremenok, Semiconductors, 43, 96 (2009); https://doi.org/10.1134/S1063782609010199
[19] D. U. Ngbiche, I. Nkrumah, F. K. Ampong, M. Paal, R. K. Nkum, F. K. Boakye, Open Journal of Applied Sciences 9, 785 (2019); https://doi.org/10.4236/ojapps.2019.911064
[20] D. B. Puzer, I. Nkrumah, F. K. Ampong, M. Paal, E. A. Botchway, R. K. Nkum, F. Boakye, Chalcogenide Letters 18(8), 481 (2021); https://doi.org/10.15251/CL.2021.188.481
[21] A. S. Hassanien, I. Sharma, Optik 200, 163415 (2020); https://doi.org/10.1016/j.ijleo.2019.163415